NeuroImage: Clinical 32 (2021) 102856

Contents lists available at ScienceDirect

NeuroImage: Clinical

journal homepage: www.elsevier.com/locate/ynicl

Wavelet-based neurovascular coupling can predict brain abnormalities in neonatal encephalopathy

Yudhajit Das [a], Rachel L. Leon [b], Hanli Liu [a], Srinivas Kota [c], Yulun Liu [d], Xinlong Wang [a], Rong Zhang [e], Lina F. Chalak [b,*]

[a] Department of Bioengineering, University of Texas at Arlington, Arlington, TX, USA
[b] Department of Pediatrics, University of Texas Southwestern Medical Center, Dallas, TX, USA
[c] Department of Neurological Surgery, University of Texas Southwestern Medical Center, Dallas, TX, USA
[d] Department of Population and Datasciences, University of Texas Southwestern Medical Center, Dallas, TX, USA
[e] Departments of Neurology and Internal Medicine, University of Texas Southwestern Medical Center, Dallas, TX, USA

ARTICLE INFO

Keywords:
Neurovascular coupling
Wavelet coherence analysis
Neonatal EEG analysis
Amplitude-integrated EEG
Near infrared spectroscopy
Hypoxic-ischemic encephalopathy

ABSTRACT

Background: Hypoxic-ischemic encephalopathy (HIE) is a leading cause of morbidity and mortality in neonates, but quantitative methods to predict outcomes early in their course of illness remain elusive. Real-time physiologic biomarkers of neurologic injury are needed in order to predict which neonates will benefit from therapies. Neurovascular coupling (NVC) describes the correlation of neural activity with cerebral blood flow, and the degree of impairment could predict those at risk for poor outcomes.

Objective: To determine if neurovascular coupling (NVC) calculated in the first 24-hours of life based on wavelet transform coherence analysis (WTC) of near-infrared spectroscopy (NIRS) and amplitude-integrated electroencephalography (aEEG) can predict abnormal brain MRI in neonatal HIE.

Methods: WTC analysis was performed between dynamic oscillations of simultaneously recorded aEEG and cerebral tissue oxygen saturation (SctO2) signals for the first 24 h after birth. The squared cross-wavelet coherence, R^2, of the time–frequency domain described by the WTC, is a localized correlation coefficient (ranging between 0 and 1) between these two signals in the time–frequency domain. Statistical analysis was based on Monte Carlo simulation with a 95% confidence interval to identify the time–frequency areas from the WTC scalograms. Brain MRI was performed on all neonates and classified as normal or abnormal based on an accepted classification system for HIE. Wavelet metrics of % significant SctO2-aEEG coherence was compared between the normal and abnormal MRI groups.

Result: This prospective study recruited a total of 36 neonates with HIE. A total of 10 had an abnormal brain MRI while 26 had normal MRI. The analysis showed that the SctO2-aEEG coherence between the group with normal and abnormal MRI were significantly different ($p = 0.0007$) in a very low-frequency (VLF) range of 0.06–0.2 mHz. Using receiver operating characteristic (ROC) curves, the use of WTC-analysis of NVC had an area under the curve (AUC) of 0.808, and with a cutoff of 10% NVC. Sensitivity was 69%, specificity was 90%, positive predictive value (PPV) was 94%, and negative predictive value (NPV) was 52% for predicting brain injury on MRI. This was superior to the clinical Total Sarnat score (TSS) where AUC was 0.442 with sensitivity 61.5%, specificity 30%, PPV 75%, and NPV 31%.

Conclusion: NVC is a promising neurophysiological biomarker in neonates with HIE, and in our prospective cohort was superior to the clinical Total Sarnat score for prediction of abnormal brain MRI.

1. Introduction

Birth asphyxia remains a serious clinical burden that affects over 1 million newborns worldwide each year (Kurinczuk et al., 2010) and the resultant hypoxic–ischemic encephalopathy (HIE) is an important cause of neurodevelopmental impairment, long-term disability, and death (Thornberg et al., 1995; Volpe, 2012). Asphyxia impairs fetal cerebral blood flow and is manifested after birth by a distinctive neonatal

* Corresponding author.
E-mail address: Lina.chalak@utsouthwestern.edu (L.F. Chalak).

https://doi.org/10.1016/j.nicl.2021.102856
Received 28 January 2021; Received in revised form 24 September 2021; Accepted 12 October 2021
Available online 20 October 2021

encephalopathy (NE), which is usually classified using the clinical Sarnat staging. Initiation of TH improves outcome by reducing the risk of cerebral palsy and significant disability in infants born with moderate and severe HIE (Jacobs, 2013; Azzopardi et al., 2014). Currently, the neurologic exam in the setting of a perinatal event is the only method to identify neonates with HIE, determine their degree of encephalopathy, and select those candidates who are within six hours of birth for the only approved treatment, therapeutic hypothermia (TH). A key clinical challenge is the initial difficulty to discern the encephalopathy severity within a short therapeutic window for the initiation of hypothermia treatment (Gluckman et al., 2005; Zhou, 2010; Jacobs, 2011). New compelling data indicates that 30–50% of newborns errounously labelled with mild HIE using the early clnical classification will have developmental delays. This stems from the fact that we are currently unable to classifiy infants at risk with the examination alone to identify which neonates are at highest risk for adverse outcomes (Chalak et al., 2018; Finder et al., 2020). Early physiological biomarkers that are immediately obtainable in the first day of life to predict which neonates with mild HIE need therapy are highly needed.

Brain MRI with spectroscopy is a validated biomarker of neurodevelopmental outcome at 18–24 months of age, but is not typically performed until 5 days of life, following the completion of TH. A key gap exists in identifying neonates at risk for poor outcomes earlier in their course in order to direct clinical care. The discovery and validation of dynamic real-time biomarkers to guide decision making regarding appropriate candidate selection for TH and the evolving landscape of adjuvant treatments has the potential to improve both prognostication and clinical care for neonates with HIE.

Continuous neuromonitoring tools are commonly used in the NICU for encephalopathic newborns during TH to assess brain function, including electroencephalography (EEG), amplitude-integrated EEG (aEEG), and near infrared spectroscopy (NIRS) (Toet et al., 2002; Hellstrom-Westas et al., 1995; Meek, 1999; van Bel, 1993). Although regular bedside monitoring is important for identifying brain injury (Peng, 2015; Shellhaas et al., 2013) the predictive abilities are typically more reliable within 24 hours (Ouwehand, 2020; Thoresen et al., 2010; Ancora et al., 2013). Various factors contribute to this, such as the fluctuating degree of encephalopathy, the complex etiology and uncertain timing of the neurologic injury (Thoresen et al., 2010; Sabir and Cowan). As a solution to this problem, we have developed an advanced quantitative analysis of data simultaneously-collected from NIRS and EEG to measure the coupling of brain function (EEG) and cerebral blood flow (NIRS) in the newborn. The goal of the newly proposed adjunct biomarkers is to improve decision making regarding candidacy for TH in the first day of life (DOL) as well as to prognosticate abnormal imaging and neurodevelopmental outcomes.

In a prior proof of concept cohort of infants with moderate to severe HIE who were receiving TH, we reported that the novel wavelet transform coherence analysis of neurovascular coupling (WTC-NVC) obtained throughout the 72 h of hypothermia can accurately identify infants with abnormal neurodevelopmental outcomes at 18–24 months (Chalak et al., 2017). Our aims in this current prospective study are to test the WTC-NVC obtained in the first DOL in a validation cohort with HIE to determine whether WTC-NVC can 1) predict infants who develop MRI brain injuries, and 2) compare its predictive value with Total Sarnat scoring in the first 6 h of life.

2. Methods

2.1. Study population and measurement protocol

The study was approved by the Institutional Review Board of the University of Texas Southwestern Medical Center and informed consent was obtained from parents before enrollment. Inclusion criteria were 1) evidence of an acute perinatal event, fetal metabolic acidosis, and an exam indicative of encephalopathy, 2) birthweight $\geq$ 1800 g, and 3) gestational age at birth $\geq$ 36 weeks. Infants admitted to the NICU at Parkland Memorial Hospital, Dallas, TX during the study period between March 2018 and February 2019 were screened for eligibility. For enrolled infants, neuromonitoring was initiated within six hours of birth and continued for a duration of 24 h. Electroencephalogram (EEG) and regional near infrared spectroscopy-based cerebral tissue oxygen saturation (NIRS-SctO2) were simultaneously recorded during the entire course of monitoring.

2.2. Encephalopathy severity classification

The severity of encephalopathy in neonates was graded based on the modified Sarnat exam performed within the first six hours of life (Sarnat and Sarnat, 1976; Sarnat et al., 2020). The resultant Total Sarnat score (TSS) was based on evaluation in the following areas: level of consciousness, spontaneous activity, posture, tone, primitive reflexes (suck, moro), and the autonomic nervous system (pupils, heart rate, respiration) (Sarnat and Sarnat, 1976; Lipper et al., 1986).

2.3. Neuroimaging assessments

All study infants underwent structural brain MRI and MR spectroscopy on a 3 Tesla MRI scanner (Philips Healthcare Systems, TX) at a median age of 5 days to evaluate for evidence of neurologic abnormalities. MRI findings were scored for abnormalities by an experienced pediatric neuro-radiologist based on the National Institute of Child Health and Human Development (NICHD) MRI-classification criteria which describes HIE-related neurologic injury involving white matter with or without extension to the cortical areas or deep gray nuclei, and/or injury involving the the basal ganglia or thalamus (BGT) (Chalak, 2014; Rollins, 2014).

2.4. EEG and NIRS data preprocessing

EEG data were acquired from eight electrodes placed on each newborn's scalp at C3, C4, P3, P4, O1, O2, Cz, and Fz locations, according to the 10–20 international system.. EEG signals were recorded at a sampling rate of 256 Hz and then amplified and filtered within a frequency band of 0.1–100 Hz. Regional SctO2 was measured on each neonate's forehead using an INVOS™ 4100–5100 oximetry (Somanetics, Troy, MI) and a neonatal sensor at a sampling rate of 0.21 Hz. Both EEG and NIRS-SctO2 signals were interfaced with a multi-device synchronization platform (Moberg Research, Inc., PA, USA) for simultaneous recording of two modalities and then saved for off-line analysis using MATLAB (Mathworks, Inc., MA, USA). For this specific study, the time series of EEG from a cross-hemisphere electrode pair of C3 and C4 (i.e., two electrodes in the central region) were used for data analysis of all the neonates. The EEG data from C3-C4 channel pair were first passed through an asymmetric band-pass filter (Parks-McClellan linear-phase FIR filter), which strongly attenuated the signal below 2 Hz and above 15 Hz, followed by conversion to aEEG using Washington University-Neonatal EEG Analysis Toolbox (WU-NEAT) (Vesoulis et al., 2020; Das et al., 2020). Artificial spikes from aEEG data were first detected and interpolated with neighboring data points. The resultant aEEG and raw NIRS signal were then detrended, and thresholded to suppress any speckle noise present in the data. Both the time series were further inspected to identify artifacts, which were removed by linear interpolation between neighboring data points, followed by a second-order polynomial de-trending to remove the slow drifts of each time series. On an average, 4.75 percent of time series data was interpolated for each subject as a part of the artifact removal procedure.

2.5. Wavelet coherence analysis

We used a MATLAB-based software package and analytic Morlet wavelet to perform WTC analysis (Grinsted et al., 2004) between the

spontaneous oscillations of artifact-free NIRS-SctO2 and aEEG signals in neonates with encephalopathy, as reported in our recent publications (Das et al., 2020; Tian et al., 2016; Tian, 2020). WTC is a time–frequency domain analysis and characterizes the squared cross-wavelet coherence, R^2, and relative phase, $\Delta\phi$, between two time series at multiple time scales and over the entire time duration, without a prior assumption of linearity and stationarity. R^2 can be conceptualized as a localized correlation coefficient (ranging between 0 and 1) between these two signals in the time–frequency domain. The statistical significance of R^2 is estimated based on Monte Carlo simulation with a 95% confidence interval to identify the R^2 regions that are statistically significant against simulated background noise ($p < 0.05$) (Maraun and Kurths, 2004). All the pixels which have statistically significant coherence values are marked as black contours within the time-scale map. Using a time-scale (equivalent to time–frequency) domain, NVC was assessed by percentage of the number of significant pixels (Pix_{sig}) over the number of total pixels (Pix_{total}) within the given time-scale map (Das et al., 2020; Tian et al., 2016; Tian, 2020), namely, Pix_{sig}/Pix_{total}. Specifically, Pix_{sig} and Pix_{total} were quantified by summing pixel numbers across all wavelet time scales only within the identified contours and all scales respectively. The percentage of significant coherence between SctO2 and aEEG was quantified across all phase ranges.

3. Results

3.1. Demographics of the study cohort

Thirty-six neonates were enrolled following parental consent. Brain MRI was abnormal in 10 infants (28%) and normal in 26 infants (72%). Abnormal brain MRIs showed injuries consistent with HIE including white matter and basal ganglia abnormalities. In the overall cohort Gestational age was 39 ± 1.4 weeks, 58% were males, Apgar at 1 min had median of 2 [interquartile range (IQR) 1, 3], Apgar at 5 min was 5 [IQR 4, 7] and cord umbilical pH showed severe fetal acidosis mean 7 ± 0.1, base deficit 17.4 ± 6.7. MRI was performed on all infants on median day of life 5 [IQR 4, 7] (Table 1). The Sarnat examination performed in the first 6 h of life identified 15 with mild, 18 with moderate, and 3 with severe encephalopathy. Notably, the incidence of abnormal MRI findings was similar in those with mild vs. moderate encephalopathy in the first 6 h.

Table 1
Characteristics of the Study Cohort.

Neonatal Characteristics	Overall	MRI		*P* value
		Normal	Abnormal	
Total N	36	26	10	
Male: N (%)	21 (58%)	14 (54%)	7 (70%)	0.468
Gestational Age (weeks)				
Mean (SD)	39 (1.4)	39 (1.3)	39 (1.9)	0.857
Median [IQR]	39 [38 40]	39 [38 39]	39 [37 40]	
Birth Weight (kg), mean (SD)	3.3 (0.7)	3.4 (0.8)	3.2 (0.6)	0.422
Maternal Race/Ethnicity: N (%)				0.644
Caucasian non-hispanic	2 (6%)	1 (4%)	1 (10%)	
Black non-hispanic	6 (17%)	4 (15%)	2 (20%)	
Hispanic	25 (69%)	18 (69%)	7 (70%)	
Other non-hispanic	3 (8%)	3 (12%)	0	
Maternal Risk Factors: N (%)				
Hypertension	9 (25%)	6 (23%)	3 (30%)	0.686
Diabetes	3 (8%)	2 (8%)	1 (10%)	1.000
Pre-eclampsia	11 (31%)	9 (35%)	2 (20%)	0.688
Labor Complications: N (%)				
Meconium	9 (25%)	8 (31%)	1 (10%)	0.392
Umbilical Cord Prolapse	1 (3%)	0	1 (10%)	0.278
Placental Abruption	4 (11%)	1 (4%)	3 (30%)	0.057
Uterine Rupture	3 (8%)	2 (8%)	1 (10%)	1.000
Maternal Chorioamnionitis	11 (31%)	8 (31%)	3 (30%)	1.000
Placental Chorioamnionitis	19 (58%)	16 (67%)	3 (30%)	0.122
Delivery Mode: N (%)				0.709
Caesarean	21 (58%)	16 (62%)	5 (50%)	
Vaginal	15 (42%)	10 (38%)	5 (50%)	
Apgar 1 min, median [IQR]	2 [13]	2 [14]	1 [12]	0.079
Apgar 5 min, median [IQR]	5 [47]	6 [47]	4 [16]	0.134
Umbilical Cord Gas pH	7.0 (0.1)	7.0 (0.1)	7.0 (0.2)	0.437
Base Deficit	17.7 (6.1)	16.7 (5.7)	20.3 (6.6)	0.172
Encephalopathy Grade: N (%)				0.336
Mild	15 (42%)	11 (42%)	4 (40%)	
Moderate	18 (50%)	14 (54%)	4 (40%)	
Severe	3 (8%)	1 (4%)	2 (20%)	
DOL at MRI, median [IQR]	5 [47]	5 [47]	5 [56]	0.892
Disposition:				
DOL at discharge, median	10 [619]	10 [620]	10 [714]	0.958
Death prior to discharge	2 (6%)	0	2 (20%)	0.071

3.2. NVC of infants with and without abnormal MRI outcomes

Neonates were divided based on their MRI brain findings. Group 1 comprised of 26 neonates having a normal brain MRI; group 2 comprised of 10 neonates with abnormal MRI brain with HIE patterns of injury including white matter injury, basal ganglia (BG) injury, and watershed infarcts. Fig. 1 shows examples of two sets of data, one from an infant with normal MRI (Figs. A–d), and the other from an infant with evidence of injury in the basal ganglia (Figs. E–h). Each are displayed with the corresponding 20-hour simultaneous recordings of aEEG and SctO2 obtained in the first DOL prior to the MRI. Fig. 1(a) shows the tracing with normal sleep-awake cycle and continuous voltage range throughout the recording, with upper and lower aEEG margins > 10 μV and > 5 μV, respectively, and the SctO2 recorded across 20 h (mean 79%). Fig. 1(b) provides time–frequency spectrograms of corresponding aEEG and SctO2, from (a), where the x-axis represents time in hour, the y-axis represents scale in minute, and the color scale represents the amplitude of power after continuous wavelet transform (CWT). Fig. 1(c) plots the WTC-based time-scale (equivalently to time–frequency) map to represent aEEG and SctO2 coupling or coherence (i.e., NVC), with the coherence range between 0 and 1, as marked by color. Fig. 1(d) presents an axial T1 image of the normal brain MRI from the infant.

In a similar format, Fig. 1(e–h) illustrate a newborn who had abnormal MRI before discharge with white matter subcortical injury accompanied by subtle diffusion restriction and basal ganglia changes as highlighted in Fig. 1(h). Fig. 1(e) indicates similar overall visual trends in aEEG and SctO2 at the bedside with mean SctO2 of 81%. Fig. 1(f) illustrates two time-scale spectrograms of aEEG and SctO2. Fig. 1(g) shows a corresponding WTC-based time-scale map for the infant with brain abnormality and Fig. 1(h) shows the abnormal brain anatomy. In contrast to the visual analysis with no distinct patterns, the time-scale spectrograms from aEEG and SctO2 time series of the normal neonate is evenly distributed across time (Fig. 1b), whereas Fig. 1(f) shows different trends starting around 10 h. The neonate with normal MRI had significantly higher WTC coherence of NVC compared to the newborn with abnormal MRI, observed specifically in the scale range of 16–250 min Fig. 1(c) and (g).

At the group level, analysis of all newborns was performed in Fig. 2 showing the 26 neonates with normal MRI and 10 neonates with abnormal MRI. The exact Wilcoxon Rank Sum test performed showed significant difference in SctO2 vs. aEEG coherence between groups ($p = 0.0007$) within the wavelet scale of 64–250 min, equivalent to very low-frequency (VLF) range of 0.06–0.2 mHz.

3.3. Correlation between NVC and Total encephalopathy severity score (TSS)

Next, we investigated the TSS relationship with percent NVC in the first DOL. The TSS provides a numerical score of encephalopathy using the 7 subcategories of the Sarnat exam, with higher scores indicating greater degree of encephalopathy (Sarnat and Sarnat, 1976; Walsh, 2017; Chalak et al., 2019). Fig. 3(a) shows the relationship between TSS

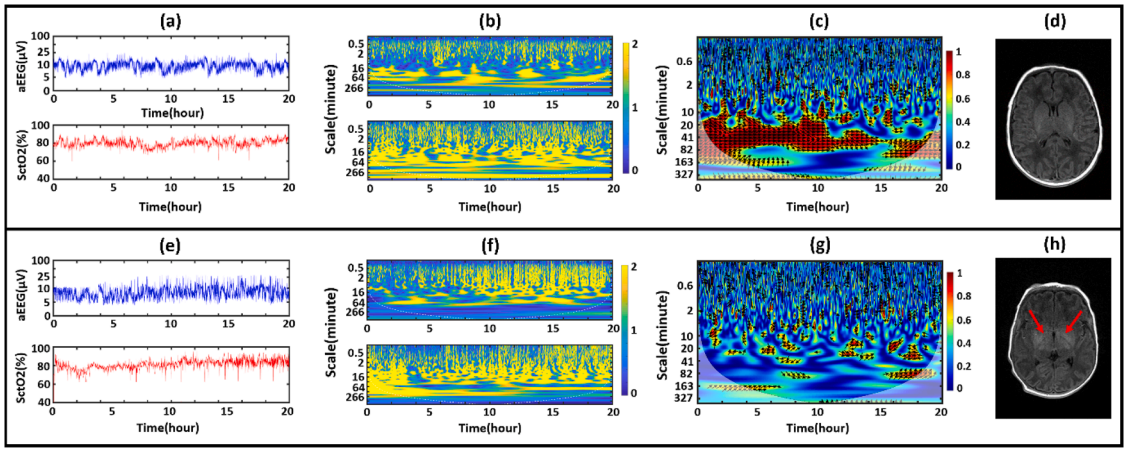

Fig. 1. Illustration of data from one neonate with normal MRI (top row of panels) and one neonate with abnormal MRI (bottom row of panels). (a & e) Examples of simultaneously recorded 20-hour aEEG (in μV) and SctO2 (in %) tracings with a sampling rate of 0.21 Hz. (b & f) Continuous wavelet transform (CWT) of the corresponding tracings from (a) and (e), where y-axes represent the scale in minute and the color gradient represents the amplitude of power after CWT. (c & g) Time-scale coherence maps of NVC of the selected infants; x-axis in all panels represents time in hour; y-axes represent scale in minute; color gradient scale indicates the amplitude of WTC coherence, R^2. The areas with significant NVC ($p < 0.05$) are red. (d & h) T1 weighted axial brain MRI slices obtained on day 5 of life. Arrows in (h) indicate the basal ganglia abnormalities consistent with HIE. (For interpretation of the references to color in this figure legend, the reader is referred to the web version of this article.)

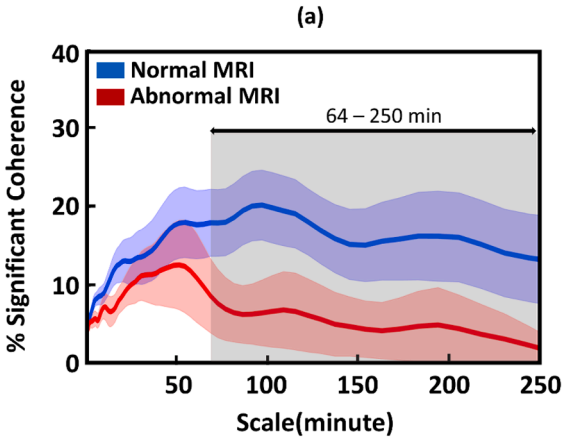

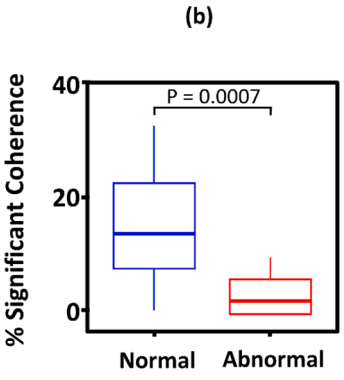

Fig. 2. (a) Mean percentages of significant coherence of SctO2 and aEEG from newborns with normal MRI outcome (n = 26; shown in blue) and abnormal MRI brain (n = 10; shown in red), based on NICHD classification of MRI in HIE. The blue and red shaded regions represent the standard errors of the mean for the respective groups. Significant differences between normal and abnormal groups ($p < 0.05$) were observed in the selected wavelet scale range of 64–250 min (a). Boxplot (median, 25% and 75% percentiles) representation for the % NVC coherence across all phases showed 95% significance with ($p = 0.0007$) by Exact Wilcoxon Rank Sum test (b). (For interpretation of the references to color in this figure legend, the reader is referred to the web version of this article.)

and percent NVC in neonates with HIE in the first DOL. A horizontal dotted line at TSS of 5 highlights the empirical TSS threshold to identify or separate neonates with a higher risk of developing abnormality. A vertical dotted line at 10% marks WTC-based NVC decision threshold to separate neonates with HIE with the highest potential of having brain abnormalities by MRI. Receiver operating characteristic (ROC) curves are plotted in Fig. 3(b) for TSS (represented in orange) and NVC (represented in green). NVC area under the curve (AUC) was 0.808, with a sensitivity of 69%, a specificity of 90%, positive predictive value (PPV) 94%, and negative predictive value (NPV) 52% for predicting brain injury on MRI. For the TSS, AUC is 0.442, sensitivity is 61.5%, specificity was 30%, PPV was 75%, and NPV was 31%. Overall, Fig. 3 highlights that a cutoff of 10% NVC during the first DOL showed higher sensitivity, specificity, PPV, and NPV compared to TSS for predicting brain injury on MRI.

In exploratory analyses, the subsets of neonates classified as 'mild' (top panel, a and b) and 'moderate' HIE (bottom panel, c and d) were further evaluated in Fig. 4, since those two groups are the most difficult to distinguish clinically. Fig. 4 (a and c) show the mean percentage of significant coherence between SctO2 and aEEG in the 15 neonates with mild (Fig. 4a) and 14 with moderate (Fig. 4c) HIE. Neonates with abnormal MRI, irrespective of their initial classification of the encephalopathy grade as 'mild' (Fig. 4b) or 'moderate' (Fig. 4d), exhibit a common pattern of lower NVC when compared to newborns with similar degree of encephalopathy and normal MRI.

4. Discussion

This study validated the utility of dynamic wavelet transform coherence analysis (WTC) to assess neurovascular coupling (NVC) in neonates with HIE who had normal brain MRI compared to those with abnormal brain MRI. We present evidence for the first time that the percent NVC in the first 24 h of life outperformed the Total Sarnat score in the ability to predict brain injuries by MRI in neonates with HIE. The clinical relevance of this study directly relates to the challenge neonatologists face in discerning mild versus moderate encephalopathy in neonates, an essential judgment in order to initiate targeted therapies. Neonates with mild NE are of particular interest, as they are not candidates for TH at most centers due to their exclusion from the major clinical trials that inform our current practice (Sarnat and Sarnat, 1976; Robertson and Finer, 1993). In our exploratory analyses (Fig. 4) we show that WTC to assess NVC is able to differentiate neonates with mild HIE and abnormal brain MRI from those with normal MRI.

In the era of developing new treatments for HIE, the NVC proposed

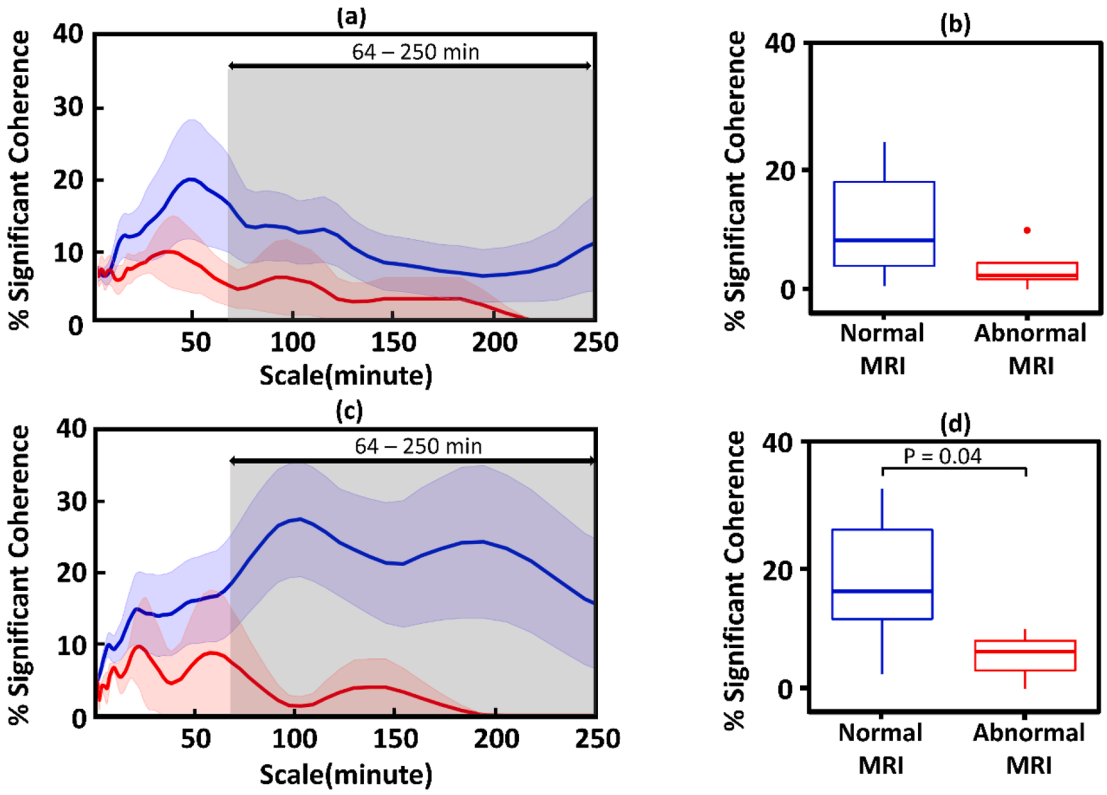

Fig. 3. (a) TSS relationship with percent NVC assessed in the first day of life of 36 HIE infants with normal (n = 26; blue dots) and abnormal (n = 10; red dots) MRI outcomes in light of their association with predicting respective brain abnormalities at a later time. (b) Receiver operator characteristic (ROC) curves for TSS (orange) and NVC (green). (For interpretation of the references to color in this figure legend, the reader is referred to the web version of this article.)

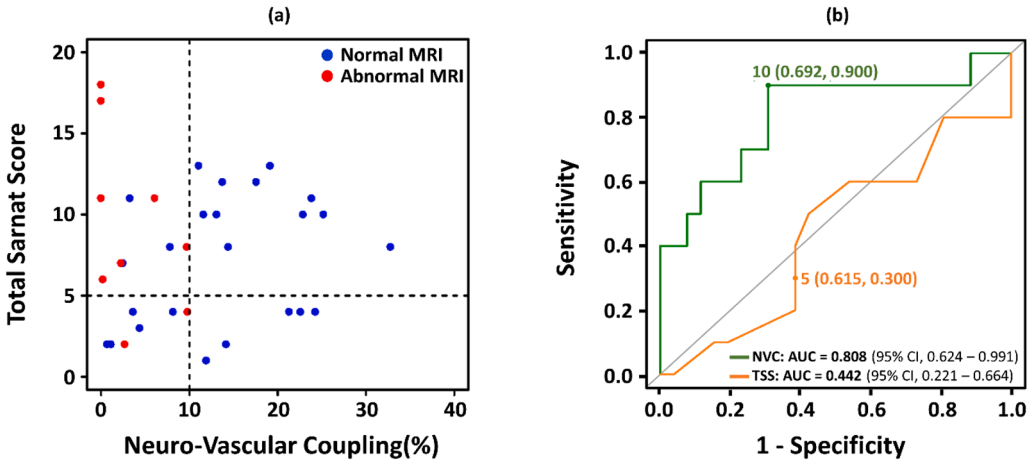

Fig. 4. (a) Mean percentage significant coherence of SctO2 vs. aEEG from 15 newborns with 'mild' HIE, 11 of whom had normal MRI outcome (shown in blue) and 4 had abnormal MRI outcome (shown in red) The shaded regions represent the standard errors of mean. (b) For the mild HIE group, statistical difference of SctO2 and aEEG coherence in the selected wavelet scale range of 64–250 min is not significant between the normal MRI vs. abnormal MRI groups. (c) Mean percentage significant coherence from 14 newborns with 'moderate' HIE, 12 of whom had normal MRI outcome (shown in blue) and 2 had abnormal MRI outcome (shown in red). The shaded regions represent the standard errors of mean. (d) For the moderate HIE group, the difference of NVC (i.e., SctO2 and aEEG coherence) in the selected scale range of 64–250 min is statistically significant (p = 0.04) between the normal and abnormal groups. (For interpretation of the references to color in this figure legend, the reader is referred to the web version of this article.)

physiological biomarker can play an essential role to provide individualized and effective additional neuroprotective and neurorestorative therapies targeting those newborns at higher risk, while sparing those at lower risk.

Clinically, the TSS is a validated score in the first six hours of life (Sarnat and Sarnat, 1976; Walsh, 2017; Chalak et al., 2019). There are six categories within the TSS, each of which is scored from 1 to 3 as as mild, moderate, or severe. Specifically, mild NE scores can range from 1 to 10, moderate NE scores range from 6 to 14, while severe scores range from 12 to 18. In a study of PRIME Prospective Research for Infants with Mild Encephalopathy, we previously demonstrated a TSS of 5 predicted abnormal neurodevelopmental outcomes at 18–22 months in mild HIE (Chalak et al., 2019). The focus of this investigation of physiological biomarkers is to solve the clinical conundrum of accurately distinguishing between those who are at risk of neurologic injury and might benefit from targeted treatments compared to those who will have normal outcomes. Our findings suggest that WTC-based NVC between aEEG-SctO2 in the first 24 h of life can successfully identify those at risk

of neurologic injury and predict an abnormal outcome.

Development in early infancy suggests that the neonatal brain may undergo complex variations in hemodynamics that differ from the adult brain (Nourhashemi et al., 2020; Roche-Labarbe et al., 2007). The hyperemic response to neuronal activation, for example, can occur within seconds, appears to be mediated by astrocytes and to be highly localized (Ariel et al., 2004).

Roy and Sherrington first introduced the NVC concept over a century ago which has been subsequently applied in modern-day neuroimaging studies of brain function with PET and functional MRI in adults (Roy and Sherrington, 1890; Aaslid, 1987; Tarapore et al., 2013). However, such techniques cannot be applied on a fragile newborn at the bedside, the reason being neither do they permit a real-time analysis of hemodynamics, because of the susceptibility to movement, nor can they measure the multi-frequency aspect of NVC as we do with the current methodology (Chalak and Zhang, 2017).

This current study used MRI-based outcomes of the neonates to evaluate the predictive abilities of WTC-based NVC between SctO2 and aEEG signals in the first DOL to predict brain injuries on DOL 5. Prior studies have shown that brain MRI prior to discharge from the hospital is a reasonable surrogate for neurodevelopmental outcomes at 2 years (Shankaran, 2015). To characterize whether MRIs were abnormal, we used the the established NICHD classification of MRI patterns of HIE which involves white matter (WM) injury extending to the cortical areas or deep gray nuclei injury in the basal ganglia or thalamus (BGT), or involvement in both areas (Barkovich, 1998; Haataja et al., 2001; Sie, et al., 2000; Miller, 2005) as these lesions are associated with impairment (Belet, et al., 2004; Steinman, 2009; van Kooij et al., 2010). Studies are ongoing to determine whether NVC between aEEG-SctO2 is predictive of long-term neurodevelopmental outcomes.

The present study highlights the utility of the WTC analysis of NVC to refine our understanding and management of HIE. Our present study utilizes a small sample size at a single center with aEEG-SctO2 coherence measured for the first 24 h of life. Additional work in larger, and ideally multi-center trials, will focus on the WTC analysis in the first 6 h of life, the critical timeframe in which neonates benefit most from initiation of TH. Adjuctive therapies for NE are currently under investigation, and the administration of these drugs may provide a wider window in the first DOL for efficacy compared to TH. These new treatments on the horizon highlight the need for additional objective data in diagnosing degree of NE, and the potential use of WTC-based analysis of NVC in clinical practice.

5. Conclusion

This novel physiological biomarker of WTC-based NVC, once validated in larger cohorts and correlated with neurodevelopmental outcomes, has significant potential to impact the early clinical stratification and prediction of brain abnormalities in neonates with encephalopathy. The ability to prospectively monitor neurovascular function in real-time, via our novel approach, could be the impetus for a paradigm shift in the field of neonatal neuro-critical care by creating precise criteria for the selection of candidates in neuroprotection studies.

Author contributions

L. C. initiated the study concept and design. Y. D. and S.K. developed MATLAB code based on the aEEG and WTC algorithm, Y.D. performed the data analysis and prepared/wrote the first draft of the manuscript. S. K. and X.W. assisted Y. D. in code debugging and modification. Y.L. performed statistical imputation and interpretation. H. L. headed the supervision of technical details and edited the manuscript. R. Z., L. C. and H. L. discussed the physiology behind application of WTC-based NVC method used in the study and interpreted the results. S.K. and R. Z. participated in interpreting the results as well as reviewed and revised the manuscript. L. C. assisted in interpreting the results, participated in manuscript writing-up and revision.

Funding

Dr. Lina Chalak is funded by NIH Grant R01NS102617.

Declaration of Competing Interest

The authors declare that they have no known competing financial interests or personal relationships that could have appeared to influence the work reported in this paper.

Acknowledgments

The study is supported by NIH Grant R01NS102617 (LC).

References

Kurinczuk, J.J., White-Koning, M., Badawi, N., 2010. Epidemiology of neonatal encephalopathy and hypoxic-ischaemic encephalopathy. Early Hum. Dev. 86 (6), 329–338. https://doi.org/10.1016/j.earlhumdev.2010.05.010.

Thornberg, E., Thiringer, K., Odeback, A., Milsom, I., 1995. Birth asphyxia: incidence, clinical course and outcome in a Swedish population. Acta Paediatr. 84 (8), 927–932.

Volpe, J.J., 2012. Neonatal encephalopathy: an inadequate term for hypoxic–ischemic encephalopathy. Ann. Neurol. 72 (2), 156–166.

Jacobs, S.E., et al., 2013. Cooling for newborns with hypoxic ischaemic encephalopathy. Cochrane database of systematic reviews.

Azzopardi, D., Strohm, B., Marlow, N., Brocklehurst, P., Deierl, A., Eddama, O., Goodwin, J., Halliday, H.L., Juszczak, E., Kapellou, O., Levene, M., Linsell, L., Omar, O., Thoresen, M., Tusor, N., Whitelaw, A., Edwards, A.D., 2014. Effects of hypothermia for perinatal asphyxia on childhood outcomes. N. Engl. J. Med. 371 (2), 140–149.

Gluckman, P.D., Wyatt, J.S., Azzopardi, D., Ballard, R., Edwards, A.D., Ferriero, D.M., Polin, R.A., Robertson, C.M., Thoresen, M., Whitelaw, A., Gunn, A.J., 2005. Selective head cooling with mild systemic hypothermia after neonatal encephalopathy: multicentre randomised trial. Lancet 365 (9460), 663–670.

Zhou, W.-H., et al., 2010. Selective head cooling with mild systemic hypothermia after neonatal hypoxic-ischemic encephalopathy: a multicenter randomized controlled trial in China. J. Pediatr. 157, 367–372.

Jacobs, S.E., et al., 2011. Whole-body hypothermia for term and near-term newborns with hypoxic-ischemic encephalopathy: a randomized controlled trial. Arch. Pediatr. Adolesc. Med. 165, 692–700.

Chalak, L.F., Nguyen, K.-A., Prempunpong, C., Heyne, R., Thayyil, S., Shankaran, S., Laptook, A.R., Rollins, N., Pappas, A., Koclas, L., Shah, B., Montaldo, P., Techasaensiri, B., Sánchez, P.J., Sant'Anna, G., 2018. Prospective research in infants with mild encephalopathy identified in the first six hours of life: neurodevelopmental outcomes at 18–22 months. Pediatr. Res. 84 (6), 861–868. https://doi.org/10.1038/s41390-018-0174-x.

Finder, M., Boylan, G.B., Twomey, D., Ahearne, C., Murray, D.M., Hallberg, B., 2020. Two-Year Neurodevelopmental Outcomes After Mild Hypoxic Ischemic Encephalopathy in the Era of Therapeutic Hypothermia. JAMA Pediatr. 174 (1), 48. https://doi.org/10.1001/jamapediatrics.2019.4011.

Toet, M.C., van der Meij, W., de Vries, L.S., Uiterwaal, C.S.P.M., van Huffelen, K.C., 2002. Comparison between simultaneously recorded amplitude integrated electroencephalogram (cerebral function monitor) and standard electroencephalogram in neonates. Pediatrics 109 (5), 772–779.

Hellstrom-Westas, L., Rosen, I., Svenningsen, N.W., 1995. Predictive value of early continuous amplitude integrated EEG recordings on outcome after severe birth asphyxia in full term infants. Arch. Dis. Child. Fetal Neonatal Ed. 72 (1), F34–F38. https://doi.org/10.1136/fn.72.1.F34.

Meek, J.H., et al., 1999. Abnormal cerebral haemodynamics in perinatally asphyxiated neonates related to outcome. Arch. Disease Childhood-Fetal Neonatal Ed. 81, F110–F115.

van Bel, F., et al., 1993. Changes in cerebral hemodynamics and oxygenation in the first 24 hours after birth asphyxia. Pediatrics 92, 365–372.

Peng, S., et al., 2015. Does near-infrared spectroscopy identify asphyxiated newborns at risk of developing brain injury during hypothermia treatment? Am. J. Perinatol. 32, 555–564.

Shellhaas, R.A., Thelen, B.J., Bapuraj, J.R., Burns, J.W., Swenson, A.W., Christensen, M. K., Wiggins, S.A., Barks, J.D.E., 2013. Limited short-term prognostic utility of cerebral NIRS during neonatal therapeutic hypothermia. Neurology 81 (3), 249–255.

Ouwehand, S., et al., 2020. Predictors of outcomes in hypoxic-ischemic encephalopathy following hypothermia: a meta-analysis. Neonatology 1–17.

Thoresen, M., Hellstrom-Westas, L., Liu, X., de Vries, L.S., 2010. Effect of hypothermia on amplitude-integrated electroencephalogram in infants with asphyxia. Pediatrics 126 (1), e131–e139.

Ancora, G., Maranella, E., Grandi, S., Sbravati, F., Coccolini, E., Savini, S., Faldella, G., 2013. Early predictors of short term neurodevelopmental outcome in asphyxiated cooled infants. A combined brain amplitude integrated electroencephalography and near infrared spectroscopy study. Brain Dev. 35 (1), 26–31.

Sabir, H., Cowan, F.M. In: Seminars in Fetal and Neonatal Medicine. pp. 15–121 (Elsevier).
Chalak, L.F., Tian, F., Adams-Huet, B., Vasil, D., Laptook, A., Tarumi, T., Zhang, R., 2017. Novel Wavelet Real Time Analysis of Neurovascular Coupling in Neonatal Encephalopathy. Sci. Rep. 7 (1) https://doi.org/10.1038/srep45958.
Sarnat, H.B., Sarnat, M.S., 1976. Neonatal encephalopathy following fetal distress. A clinical and electroencephalographic study. Arch. Neurol. 33, 696–705.
Sarnat, H.B., Flores-Sarnat, L., Fajardo, C., Leijser, L.M., Wusthoff, C., Mohammad, K., 2020. Sarnat Grading Scale for Neonatal Encephalopathy after 45 Years: An Update Proposal. Pediatr. Neurol. 113, 75–79. https://doi.org/10.1016/j.pediatrneurol.2020.08.014.
Sarnat, H.B., Sarnat, M.S., 1976. Neonatal encephalopathy following fetal distress: a clinical and electroencephalographic study. Arch. Neurol. 33, 696–705.
Lipper, E.G., Voorhies, T.M., Ross, G., Vannucci, R.C., Auld, P.A., 1986. Early predictors of one-year outcome for infants asphyxiated at birth. Dev. Med. Child Neurol. 28, 303–309.
Chalak, L.F., et al., 2014. Neurodevelopmental outcomes after hypothermia therapy in the era of Bayley-III. J. Perinatol. 34, 629–633.
Rollins, N., et al., 2014. Predictive value of neonatal MRI showing no or minor degrees of brain injury after hypothermia. Pediatr. Neurol. 50, 447–451.
Vesoulis, Z.A., Gamble, P.G., Jain, S., Ters, N.M.E., Liao, S.M., Mathur, A.M., 2020. WU-NEAT: A clinically validated, open-source MATLAB toolbox for limited-channel neonatal EEG analysis. Comput. Methods Programs Biomed. 196, 105716. https://doi.org/10.1016/j.cmpb.2020.105716.
Das, Y., Liu, H., Tian, F., Kota, S., Zhang, R., Chalak, L.F., 2020. Rigor of Neurovascular Coupling (NVC) Assessment in Newborns Using Different Amplitude EEG Algorithms. Sci. Rep. 10 (1) https://doi.org/10.1038/s41598-020-66227-y.
Grinsted, A., Moore, J.C., Jevrejeva, S., 2004. Application of the cross wavelet transform and wavelet coherence togeophysical time series. Nonlinear Processes Geophys. 11 (5/6), 561–566.
Tian, F., Tarumi, T., Liu, H., Zhang, R., Chalak, L., 2016. Wavelet coherence analysis of dynamic cerebral autoregulation in neonatal hypoxic–ischemic encephalopathy. NeuroImage: Clin. 11, 124–132.
Tian, F., et al., 2020. Regional heterogeneity of cerebral hemodynamics in mild neonatal encephalopathy measured with multichannel near-infrared spectroscopy. Pediatr. Res. 1–9.
Maraun, D., Kurths, J., 2004. Cross wavelet analysis: significance testing and pitfalls.
Walsh, B.H., et al., 2017. The frequency and severity of magnetic resonance imaging abnormalities in infants with mild neonatal encephalopathy. J. Pediatr. 187, 26–33.
Chalak, L.F., Adams-Huet, B., Sant'Anna, G., 2019. A total Sarnat score in mild hypoxic-ischemic encephalopathy can detect infants at higher risk of disability. J. Pediatr. 214, 217–221.
Robertson, C.M.T., Finer, N.N., 1993. Long-term follow-up of term neonates with perinatal asphyxia. Clin. Perinatol. 20 (2), 483–499.
Nourhashemi, M., Mahmoudzadeh, M., Goudjil, S., Kongolo, G., Wallois, F., 2020. Neurovascular coupling in the developing neonatal brain at rest. Hum. Brain Mapp. 41 (2), 503–519. https://doi.org/10.1002/hbm.v41.210.1002/hbm.24818.
Roche-Labarbe, N., Wallois, F., Ponchel, E., Kongolo, G., Grebe, R., 2007. Coupled oxygenation oscillation measured by NIRS and intermittent cerebral activation on EEG in premature infants. Neuroimage 36 (3), 718–727. https://doi.org/10.1016/j.neuroimage.2007.04.002.
Ariel, I., Anteby, E., Hamani, Y., Redline, R.W., 2004. Placental pathology in fetal thrombophilia. Hum. Pathol. 35, 729–733. https://doi.org/10.1016/j.humpath.2004.02.010.
Roy, C.S., Sherrington, C.S., 1890. On the Regulation of the Blood-supply of the Brain. J. Physiol. 11, 85–158.
Aaslid, R., 1987. Visually evoked dynamic blood flow response of the human cerebral circulation. Stroke 18 (4), 771–775.
Tarapore, P.E., Findlay, A.M., LaHue, S.C., Lee, H., Honma, S.M., Mizuiri, D., Luks, T.L., Manley, G.T., Nagarajan, S.S., Mukherjee, P., 2013. Resting state magnetoencephalography functional connectivity in traumatic brain injury. J. Neurosurg. 118 (6), 1306–1316. https://doi.org/10.3171/2013.3.JNS12398.
Chalak, L.F., Zhang, R., 2017. New Wavelet Neurovascular Bundle for Bedside Evaluation of Cerebral Autoregulation and Neurovascular Coupling in Newborns with Hypoxic-Ischemic Encephalopathy. Dev. Neurosci. 39 (1-4), 89–96. https://doi.org/10.1159/000457833.
Shankaran, S., et al., 2015. Neonatal magnetic resonance imaging pattern of brain injury as a biomarker of childhood outcomes following a trial of hypothermia for neonatal hypoxic-ischemic encephalopathy. J. Pediatr. 167, 987–993.
Barkovich, A.J., et al., 1998. Prediction of neuromotor outcome in perinatal asphyxia: evaluation of MR scoring systems. Am. J. Neuroradiol. 19, 143–149.
Haataja, L., Mercuri, E., Guzzetta, A., Rutherford, M., Counsell, S., Flavia Frisone, M., Cioni, G., Cowan, F., Dubowitz, L., 2001. Neurologic examination in infants with hypoxic-ischemic encephalopathy at age 9 to 14 months: use of optimality scores and correlation with magnetic resonance imaging findings. J. Pediatr. 138 (3), 332–337.
Sie, L.T.L., et al., 2000. MR patterns of hypoxic-ischemic brain damage after prenatal, perinatal or postnatal asphyxia. Neuropediatrics 31, 128–136 %@ 0174-0304X.
Miller, S.P., et al., 2005. Patterns of brain injury in term neonatal encephalopathy. J. Pediatr. 146, 453–460.
Belet, N., et al., 2004. Hypoxic-ischemic encephalopathy: correlation of serial MRI and outcome. Pediatr. Neurol. 31, 267–274 %@ 0887-8994.
Steinman, K.J., et al., 2009. Neonatal watershed brain injury on magnetic resonance imaging correlates with verbal IQ at 4 years. Pediatrics 123, 1025–1030.
van Kooij, B.J.M., et al., 2010. Serial MRI and neurodevelopmental outcome in 9-to 10-year-old children with neonatal encephalopathy. J. Pediatr. 157, 221–227. e222 %@ 0022-3476.